Energy and Technology Review

Lawrence Livermore Laboratory

August 1978

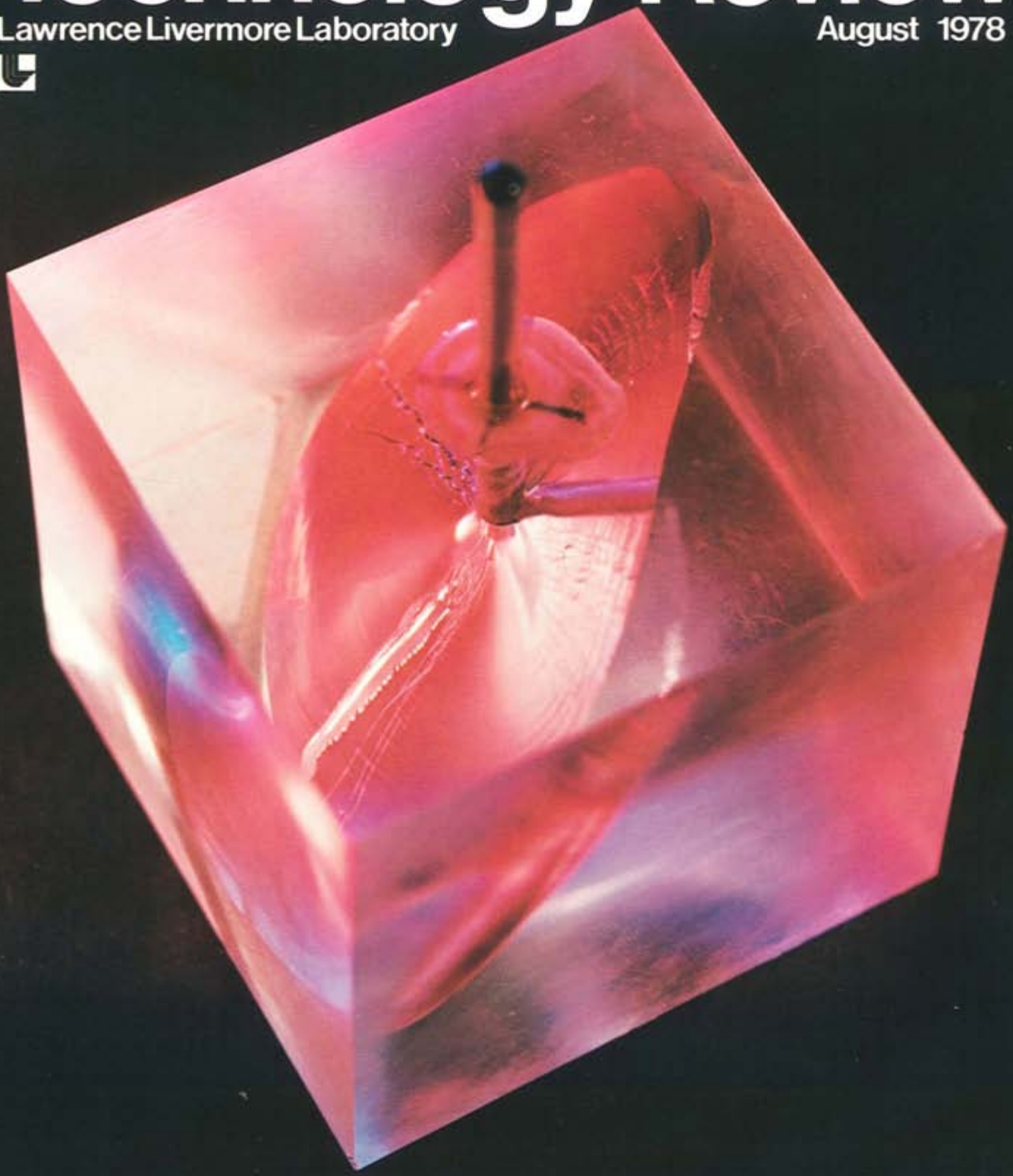

Laser–Plasma Coupling: Calculations and Experiments

To design laser fusion targets, we need a fundamental understanding of how laser light energy is absorbed and transported in matter. We have formulated analytical and simulation models that successfully describe many important features of laser–plasma coupling and that correlate well with a continuing sequence of basic target experiments.

The idea of using large, high-power lasers to compress and heat fusion fuel to thermonuclear conditions is basically very simple: a pulsed laser can focus energy onto a small target, compressing and heating the fuel inside to ignition conditions. The resulting plasma is confined by its own inertia long enough for thermonuclear reactions to take place. According to computer calculations,[1] significant target gains can be achieved—that is, the energy produced from fusion can greatly exceed the laser energy necessary to implode it. A large national effort is under way to demonstrate the feasibility of laser fusion energy.

LLL is at the forefront of this applied research effort.[2] We have a coordinated program to understand laser fusion phenomena and to implement this understanding in the design of laser fusion targets. There are five elements to our program team: plasma theorists, who use computer simulation and analytical models to investigate microscopic plasma behavior (on the scale of light- or electron-plasma wavelengths); experimentalists, who develop diagnostic instruments and conduct experiments on several laser facilities (Janus, Cyclops, Argus, and, soon, Shiva); target designers, who use the LASNEX magnetohydrodynamic code to simulate macroscopic plasma behavior (on the scale of thousands of free-space wavelengths) and to test models derived from microscopic studies; target fabricators who construct high-precision targets; and laser scientists who design and build our laser facilities.

The plasma investigation part of the laser fusion program provides a fundamental knowledge of plasma behavior and provides a basis for target design and experiments with complex, high-performance targets.

LASER–TARGET INTERACTION

To design laser fusion targets, we need to understand how laser light is absorbed and what heated-matter energies are generated. This becomes a question of how laser light couples to a plasma, since the target is very rapidly ionized by the intense light. For example, laser light with a wavelength of 1.06 μm and an intensity of 10^{15} W/cm^2 has an oscillating electric field in free space of about 10^9 V/cm, sufficient to strip an electron from an atom directly. In fact, ionization occurs at much smaller intensities (on the order of 10^{10} to 10^{11} W/cm^2) because of other effects such as cascade ionization.

One well-known property of a plasma is that it has a maximum density through which laser light

Contact William L. Kruer (422-5437) for further information on this article.

can penetrate. This electron-number density is the so-called critical density, n_{cr}, and is defined by the condition that the electron plasma frequency, ω_{pe}, equals the laser light frequency. This critical density, which is $10^{21}/\text{cm}^3$ for 1.06-μm light, is much less than solid density. Because of this, laser–plasma coupling occurs in the outer low-density matter that ablates off and surrounds the target after initial heating of the target shell (see Fig. 1).

A quantitative understanding of light–plasma coupling is one of the most challenging and difficult problems in laser fusion. As shown in Fig. 2, many different processes can compete to determine the coupling. Some of the processes lead to absorption; these include collisional heating as well as a number of processes whereby electrostatic waves are excited either linearly (resonance absorption) or nonlinearly (instabilities). Some of the processes lead to a stimulated scattering of the laser light away from the target (Brillouin or Raman instabilities, depending on whether ion-acoustic or electron-plasma waves absorb the momentum of the laser light) or lead to a modification of the intensity profile of the light beam (the self-focusing and filamentation instabilities). Once the light is absorbed, the resulting heat flow can itself drive ion turbulence and magnetic fields, which in turn modify both the absorption and the heat flow.

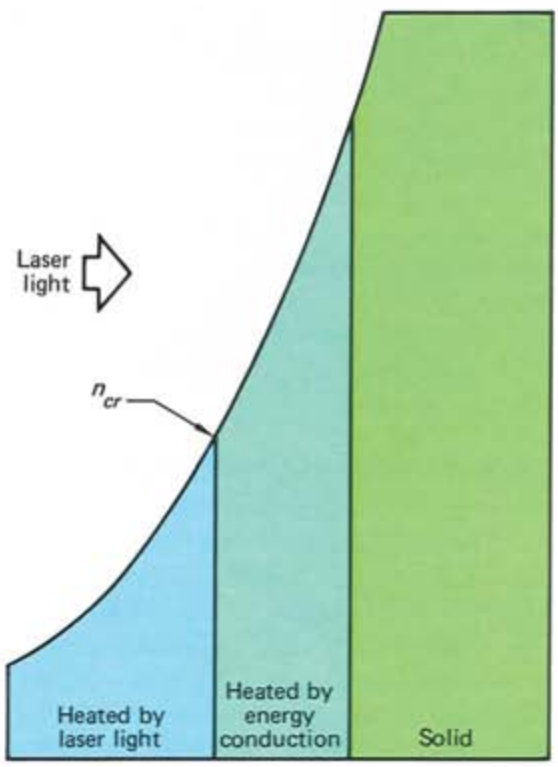

Fig. 1. Schematic of a slab target that is being irradiated with laser light. Three regions are denoted: an outer layer with density less than or equal to the critical density that is directly heated by the laser light, the underdense region; a high-density region that is heated indirectly by energy conduction; and the solid density region.

The plasma conditions depend on the mix of processes that provide the coupling; in turn, the mix of processes determines the coupling. To investigate this highly nonlinear, coupled problem, we have made extensive use of computer simulation. Our most powerful code is ZOHAR, a 2-1/2-dimensional particle simulation code (two spatial and three velocity coordinates).[3] This code models a plasma by following the motion of a large number of electrons and ions in their self-consistent electric and magnetic fields. The full set of Maxwell's equations is solved, and the particle motion is fully relativistic.

In spite of the complexity of the problem, we have made significant advances through a joint application of theory, computer simulation, and experiment. Many important results predicted by calculations have been confirmed by experiments. These include a strong density profile steepening near the critical density, polarization-dependent light absorption, suprathermal electron generation, and sizeable Brillouin scatter in long-pulse-length experiments.

DENSITY PROFILE STEEPENING

One of the fundamental results predicted by calculations performed both at LLL and LASL is a strong, nonlinear steepening of the density profile near the critical density in a laser-irradiated plasma. An early example of this steepening is shown in the Fig. 3 plot of a self-consistent density profile as computed by ZOHAR. In this case, intense laser light is obliquely incident onto a planar, expanding plasma. As the light reflects near the critical density,

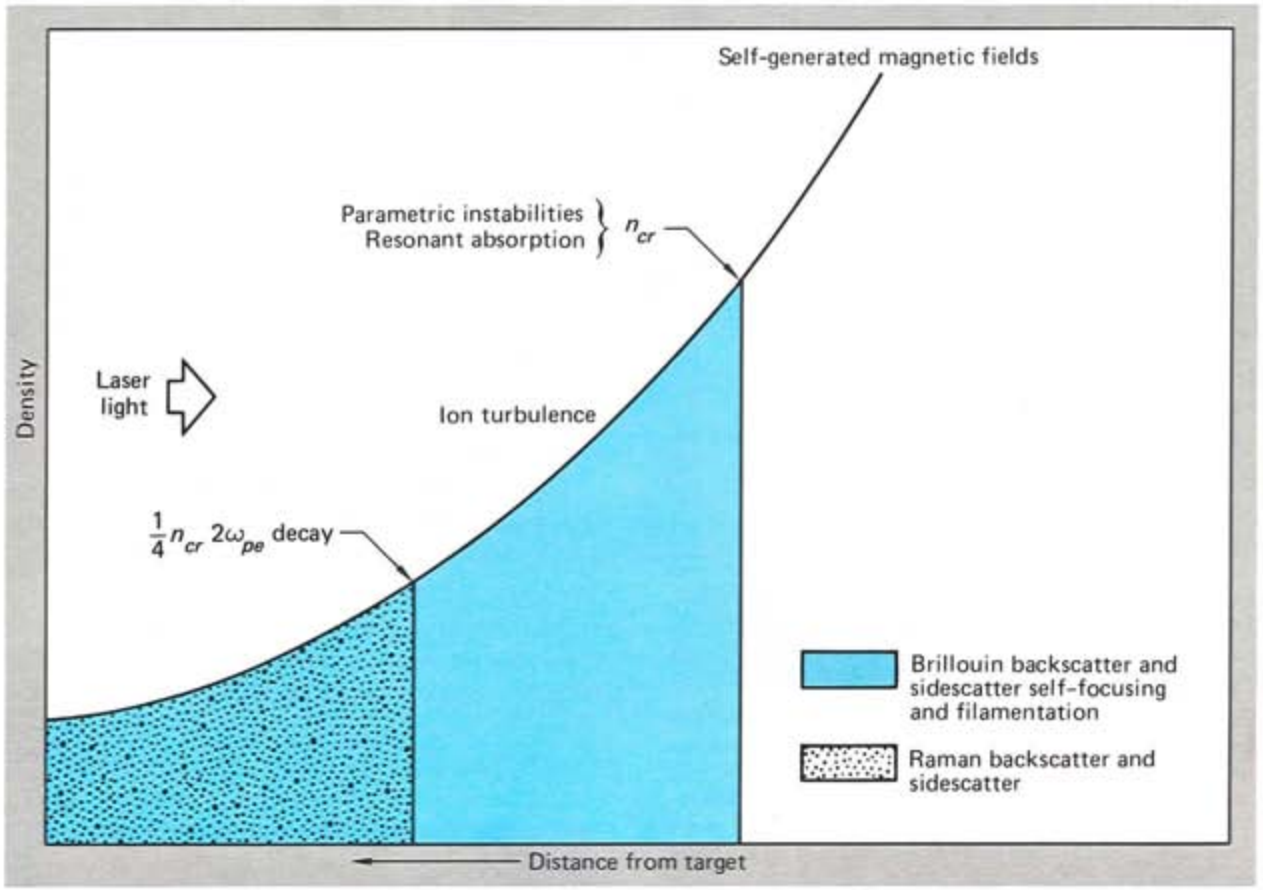

Fig. 2. **Density profile of the plasma penetrated and heated by laser light, illustrating the many physical processes that can occur.**

it is partially absorbed because of the resonant generation of electron plasma waves. The localized momentum and energy deposition then strongly steepen the density profile, leading to the self-consistent profile shown in the figure. This profile steepening has many important consequences. Resonance absorption becomes effective for a broad range of angles of incidence. Instability heating at the critical density is much reduced, and the resonantly heated electrons have lower energy. Subsequent calculations have shown that the steepening is a general phenomenon occurring wherever a localized interaction between the light and the plasma takes place.

Recently, the pronounced density profile steepening has been confirmed in our experiments on the 0.1-TW neodymium-glass laser, Janus.[4] In these experiments, part of the laser pulse was split off, frequency-doubled, and used to probe the target plasma. An interferogram was formed and the density profile reconstructed. An example is shown in Fig. 4. As expected, the profile is strongly steepened over a substantial region of densities, confirming the existence of this important effect. In both the simulations and the experiment, the plasma density is steepened to an upper density that is approximately determined by balancing the pressure of the reflecting light (about $E_L^2/4\pi$) with the plasma pressure ($n_u\theta_e$); that is,

$$n_u = n_{cr}(1 + E_L^2/4\, n_{cr}\, \theta_e)\,,$$

where E_L is the electric field of the laser light and θ_e is the background plasma temperature. The density is steepened to a lower value determined by how the light pressure dams the plasma flow. This lower density appears to be somewhat less in experiments

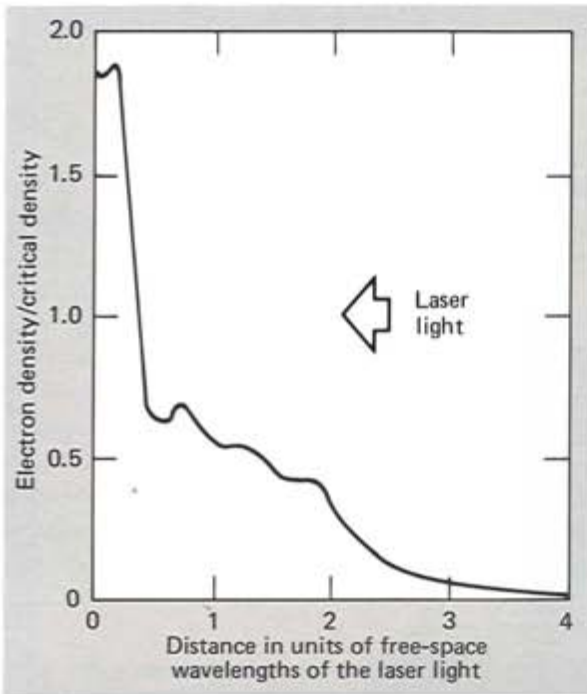

Fig. 3. **A nonlinearly steepened density profile calculated in a two-dimensional simulation of laser light absorption. In this simple example, a plane light wave is incident at an angle of 24° onto a plasma slab with an intensity of 10^{16} W/cm^2 (1.06-μm light). Initially the plasma had an electron temperature of 4 keV and a linear density profile rising to the critical density in 1.6 free-space wavelengths.**

than in our computer simulations, an effect which may be due to the inhibition of heat transport.

LASER LIGHT ABSORPTION

Calculations have also predicted many important features of the absorption in experiments with short-pulse-length, high-intensity laser light. In such experiments, the underdense plasma has both a high temperature and a small spatial extent. Because collisional absorption varies as $\theta_e^{-3/2}$ and as the scale length of the plasma, it is weak in such experiments. However, computer simulations [5] showed that there would still be sizeable absorption due to a combination of resonance absorption and heating on nonlinearly generated ion fluctuations. Resonance absorption is due to the excitation of electrostatic waves by the oscillation of electrons across a density gradient. This process occurs whenever the electric vector of the incident light has a component along the density gradient (p-polarized light) but does not occur when there is no component along the density gradient (s-polarized light). As shown in Fig. 5, the net absorption was predicted to be polarization-dependent, to be rather broad in angle, and to have typical values ranging from about 15 to 50% as a function of angle of incidence and polarization. The colored line is an early prediction based on two-dimensional particle simulations of plane waves incident on a plasma slab. The black line is the result of an improved model that incorporates additional critical surface rippling due to realistic structure in the intensity profile of the light beam.

The predictions were tested in detail by some of our recent Janus experiments. [6] In these experiments, plastic disks were irradiated with about 30-ps pulses of 1.06-μm light with an intensity of 10^{15} to 10^{16} W/cm^2. As shown in Fig. 5, the measured absorption was both polarization-dependent and broad in angle. The absorption of p-polarized light peaked at approximately the predicted angle, and the absorption of s-polarized light decreased with

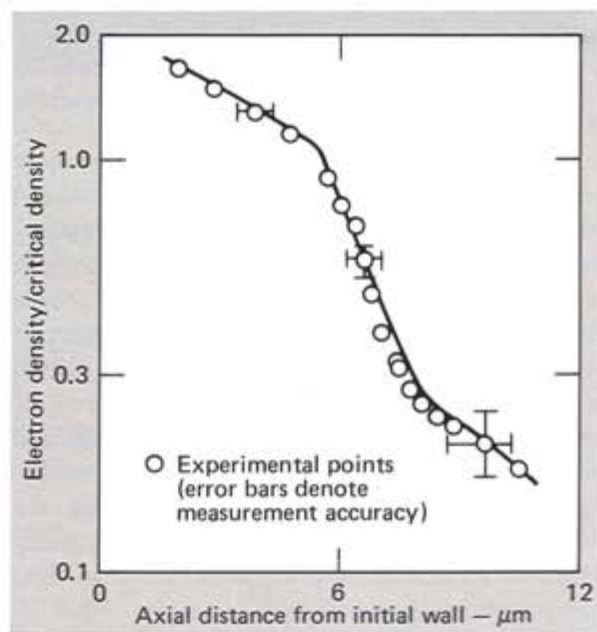

Fig. 4. **A measured density profile in a laser-irradiated target. A laser pulse with an intensity of about 5×10^{14} W/cm^2 was incident onto a glass microsphere. The profile was measured by interferometry using a frequency-doubled light pulse.**

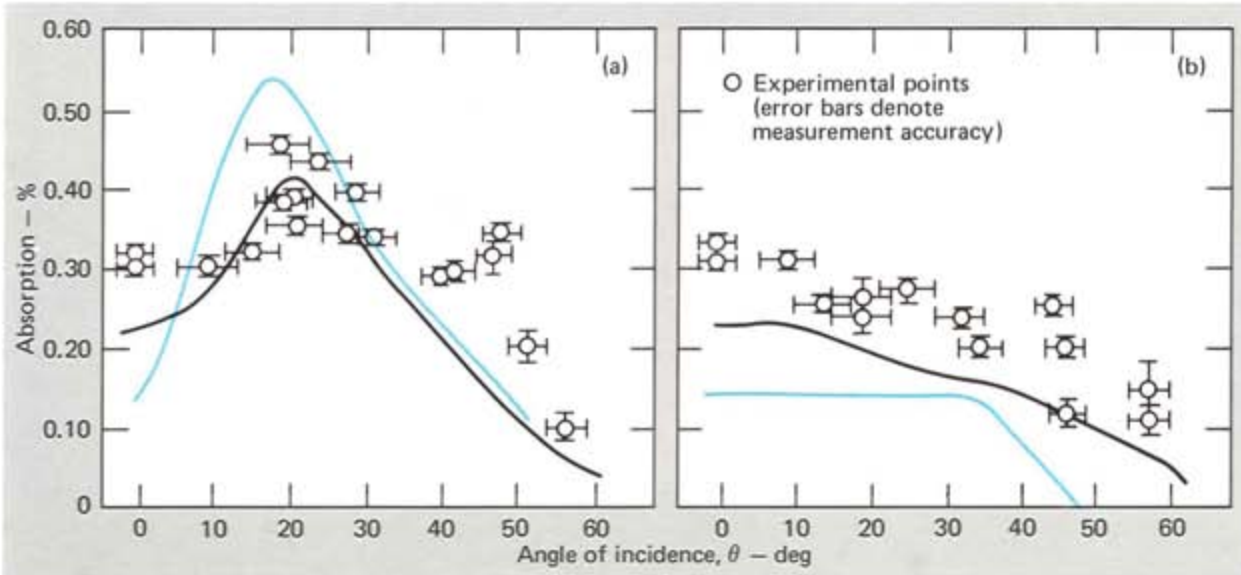

Fig. 5. **Absorption as a function of angle of incidence and polarization for (a) p-polarization and (b) s-polarization. Colored lines are based on two-dimensional computer simulations of plane waves incident onto a plasma slab. Initial plasma conditions are the same as those for Fig. 4. Black lines are obtained by modifying the plane wave results to include an additional rippling of the critical density surface due to inhomogeneities in the incident light beam. Circles denote the absorption that was measured in a series of experiments in which plastic disks were irradiated. The 1.06-μm light was focused with an $f/10$ lens to an incident intensity in the range of 10^{15} to 10^{16} W/cm^2.**

angle of incidence. The magnitude of the absorption was also in reasonable agreement. The principal discrepancy is an additional 10 to 15% absorption rather independent of angle of incidence and polarization. This additional absorption may be due to ion turbulence generated by heat-flow instabilities, self-generated magnetic fields, or the $2\text{-}\omega_{pe}$ instability.

HEATED ELECTRON ENERGIES

A very important question is the magnitude of the heated-matter energy produced. The laser light primarily heats electrons, since their motion in the oscillating fields is much greater than that of the massive ions. The ZOHAR simulations[7] predict that a two-temperature Maxwellian distribution of electrons is generated. The lower temperature is that typical of the electrons streaming into the absorption region, and the higher energy electrons are those resonantly heated by the electrostatic fields at the critical density. The hot temperature is rather weakly dependent on the laser light intensity. Typical values fall between about 3 and 50 keV for light intensities of 10^{14} to 10^{17} W/cm^2.

The existence of a two-temperature electron distribution has been confirmed in laser–plasma experiments from measurement of the x-ray spectrum emitted from the target. As shown in Fig. 6, the heated electron temperatures inferred from experiments are in reasonable agreement with those calculated over a wide intensity regime. The open circles represent measurements from a series of experiments in which plastic disks were irradiated, and the triangles denote the values calculated in two-dimensional particle simulations. As expected, the simulation values are somewhat larger because of the space- and time-averaging inherent in the experiments. Both the experiments and the simulations also indicate that the hot electron temperature increases with the Z of the target.

BRILLOUIN SCATTER

We have been discussing short-pulse-length experiments, that is, experiments characterized by a small region of plasma with density less than n_{cr}. Such experiments have been typical of the

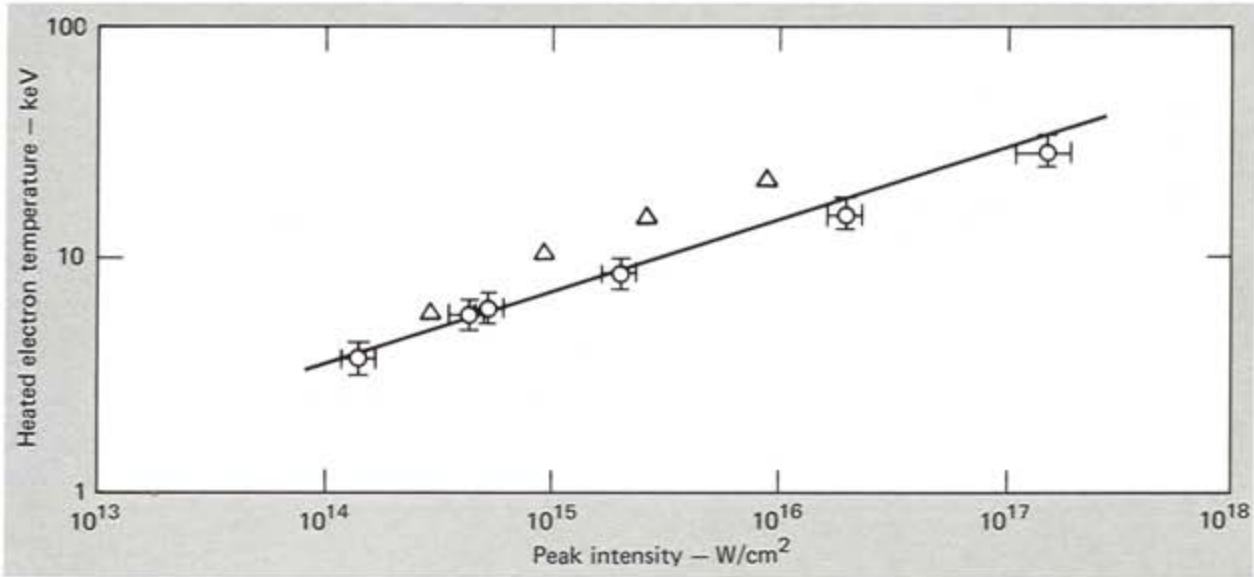

Fig. 6. The heated electron temperature as a function of intensity. The open symbols represent the values inferred from the high-energy x rays in experiments in which plastic disks were irradiated with 1.06-μm light. The triangles are values calculated in a series of two-dimensional simulations using plane waves incident onto a plasma slab.

exploding-pusher target experiments carried out in the past—early laser fusion experiments with violent nonadiabatic compression of deuterium–tritium gas to high temperature but to a density of only about 0.1 g/cm^3. Prescriptions for the calculated absorption and hot electron temperature have been incorporated into LASNEX, the target design code, and LASNEX has done rather well in tracking these implosion experiments.

Laser–plasma coupling is more difficult to compute in long-pulse-length experiments, however, because the underdense plasma is then much larger. In large regions of underdense plasma, collisional absorption, Brillouin and Raman scattering, and filamentation can all play a much more important role. The competition of these effects is poorly understood, both theoretically and experimentally.

Encouraging progress has been made in our understanding of the important role of Brillouin scattering in long-pulse-length experiments. We used both simulations and a simple theoretical model to predict sizeable Brillouin scatter in experiments with large regions of underdense plasma. As shown in Fig. 7, this backscatter was predicted to be on the order of 50% when the characteristic size of the underdense plasma is about 100 free-space laser-light wavelengths. The line is the prediction of a theoretical model for Brillouin backscatter, which takes into account the self-consistent ion heating that accompanies the instability. The squares

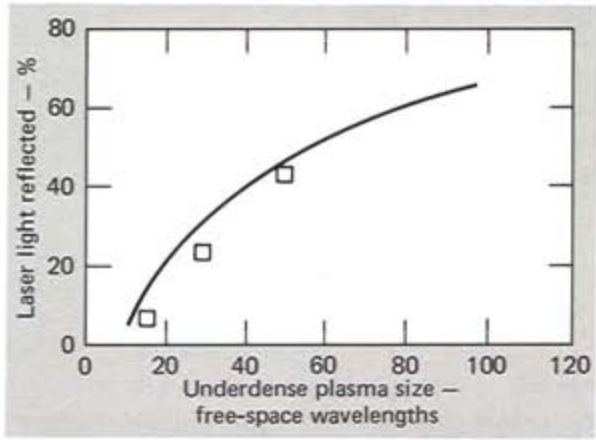

Fig. 7. The fraction of the incident light that is Brillouin-backscattered as a function of the size of a uniform underdense plasma. The line is the result of a one-dimensional theoretical model in which ion heating by the driven ion waves provides the stabilization. The squares denote simulation results using a one-dimensional code. The initial electron temperature was 2 keV; the incident light intensity was 2×10^{15} W/cm^2.

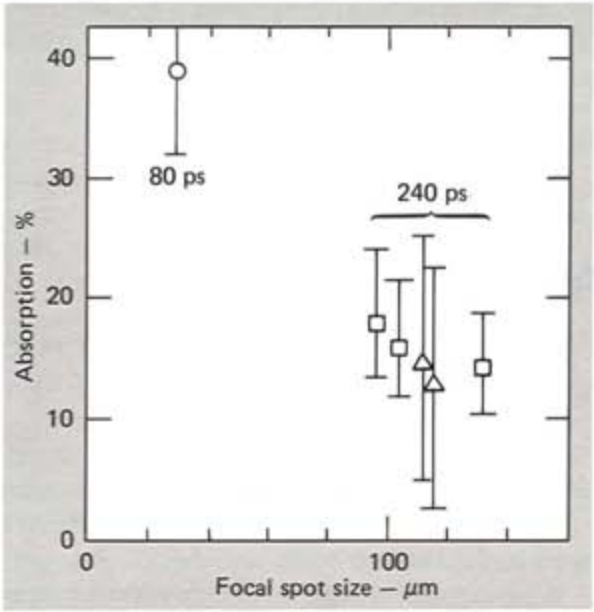

Fig. 8. **The absorption as a function of pulse length (in picoseconds) and focal spot size measured in an experiment in which plastic disks were irradiated with 1.06-μm light. The experiments with longer pulse lengths and, hence, larger regions of underdense plasma exhibited less absorption, consistent with the presence of Brillouin scatter. The laser light had an intensity in the range of 1 to 5×10^{16} W/cm^2.**

denote simulation results. Experiments[8] in which plastic disks were irradiated with neodymium light with pulse lengths of 200 to 400 ps and focused intensities of about 3×10^{15} to 3×10^{16} W/cm^2 confirmed these predictions. We found the absorption to be reduced by a factor of about two in these experiments as compared with that observed in the analogous short-pulse-length experiments (Fig. 8). Measurements of the frequency spectra of the reflected light showed red shifts characteristic of the Brillouin scatter. Subsequent long-pulse-length experiments using high-Z targets have also exhibited sizeable Brillouin scatter.

CONCLUSION

Calculations have predicted many important features of laser–plasma coupling and greatly enhanced our understanding of the fundamentals of the phenomenon. Our knowledge is most developed for short-pulse-length experiments, where resonance absorption on a rippled, steepened critical-density surface plays an important role. Long-pulse-length experimental phenomena are more difficult to decipher. Large regions of underdense plasma are created, and more plasma processes compete to determine the absorption. Brillouin scatter, for example, can play an important role, as shown in both calculations and experiments.

Key Words: laser induced fusion; plasmas—effects of laser beams; plasma heating.

NOTES AND REFERENCES

1. J. Nuckolls, L. Wood, R. Thiessen, and G. Zimmerman, *Nature* **239**, 139 (1972).
2. For an overview of LLL's laser fusion program, see the August 1977 *Energy and Technology Review* (UCRL-52000-77-8).
3. A. B. Langdon and B. F. Lasinski, in *Methods in Computational Physics*, J. Killeen, B. Alder, S. Fernbach, and M. Rotenberg, Eds. (Academic Press, New York, 1976), Vol. 16, p. 327.
4. D. T. Attwood, D. W. Sweeney, J. M. Auerbach, and P. H. Y. Lee, *Phys. Rev. Letters* **40**, 184 (1978).
5. K. Estabrook, E. J. Valeo, and W. L. Kruer, *Phys. Fluids* **18**, 1151 (1975).
6. K. R. Manes et al., *Phys. Rev. Letters* **39**, 281 (1977).
7. K. Estabrook and W. L. Kruer, *Phys. Rev. Letters* **40**, 42 (1978).
8. D. W. Phillion, W. L. Kruer, and V. C. Rupert, *Phys. Rev. Letters* **39**, 1529 (1977).